Measuring Water Diffusion in Polymer Films on the Substrate by Internal Reflection Fourier Transform Infrared Spectroscopy

I. LINOSSIER,[1] F. GAILLARD,[1] M. ROMAND,[1] J. F. FELLER[2]

[1] Laboratoire de Sciences et Ingénierie des Surfaces (Equipe CNRS ERS 69), Université de Lyon 1, 69622 Villeurbanne Cedex, France

[2] Laboratoire des Polymères & Procédés, Université de Bretagne Sud, 4 Rue Jean Zay, 56325 Lorient Cedex, France

Received 4 February 1997; accepted 10 July 1997

ABSTRACT: Among the various analysis modes which can be used in FTIR spectroscopy, the internal reflection mode enables us to gain near-surface information on solids or liquids. The interaction between the evanescent field created upon internal reflection of the infrared beam and a sample can be used to monitor the uptake of water molecules by a polymeric film. In this technique, a polymer film of sufficient thickness is applied to a substrate and a special cell is used to study the water diffusion in the polymer films. Spectra were taken automatically at specified time intervals without disturbing either the specimen or the instrument. Results for polystyrene and poly(methyl methacrylate) films applied to a ZnS substrate are presented to demonstrate the method. The diffusion coefficients of water in these polymers are calculated using the sorption kinetics approach, and the diffusion process in each type of polymer is discussed. The effects of the molecular weight and defects in the films on water transport in the polymers are illustrated. © 1997 John Wiley & Sons, Inc. J Appl Polym Sci **66:** 2465–2473, 1997

Key words: MIR-FTIR spectroscopy; water diffusion; glassy polymer films

INTRODUCTION

When a molecule diffuses through a polymer film, it is interesting to follow its in-depth distribution as a function of time in order to determine the diffusion mode. Several recent papers[1–4] have dealt with diffusion in polymer films and various classes of diffusion have been identified. Generally, the Fickian diffusion of solvents into polymers (case I) is characterized by a relaxation of the polymer, which is fast in comparison with displacement speed of the solvent front. A non-Fickian diffusion (case II) is characterized by a sharp concentration profile and a relaxation of the polymer, which is slow when compared to the rate of the diffusion front. The differentiation between Fickian and non-Fickian behaviors is not clear and some polymers follow pseudo-Fickian[5] behavior.

Diffusion coefficients of small molecules in amorphous polymers are readily measured by the use of gravimetric techniques.[6] Fixed boundary conditions are maintained and the approach to equilibrium is monitored as the polymer takes up the diffusant. When the system obeys the second Fick law, the plots of mass gained versus $t_{0.5}$ (t = time) are linear for short duration, and eventually reach some equilibrium sorption level for longer times.

For a plane film geometry, the diffusion coefficient D may be obtained from the half sorption time ($t_{0.5}$), and the film thickness,[7] $2L$:

Correspondence to: J. F. Feller.

Journal of Applied Polymer Science, Vol. 66, 2465–2473 (1997)
© 1997 John Wiley & Sons, Inc. CCC 0021-8995/97/132465-09

$$D = \frac{0.04909(2L)^2}{t_{0.5}}$$

In this work we have developed a nondestructive spectroscopic technique by which the uptake and diffusivity of small molecules, such as water in a polymeric coating, can be evaluated *in situ*. The corresponding experiment utilizes Fourier transform infrared spectroscopy (FTIR) in the multiple internal reflection (MIR-FTIR) commonly known as attenuated total reflection (ATR-FTIR). Infrared spectra are recorded as a function of time while uptake and water diffusion within the film proceed. By following the intensity change of some infrared absorption bands characteristic of the water molecules as a function of time, it is possible to calculate the corresponding diffusion coefficient.

The MIR-FTIR method offers many advantages over gravimetry to measure water or solvent diffusion in a polymer film. First, there is no need to blot the surfaces to remove excess liquid because the diffusion takes place *in situ*. Removing excess liquid on sample surfaces is one main experimental error associated with the gravimetric technique. Second, it is difficult to handle and measure the mass gain with good accuracy for thin films (<10 μm) by the gravimetric technique. Third, the spectroscopic method used in this article allows one to measure liquid mass uptake into polymer films having high diffusion coefficients. This cannot be done with sufficient accuracy by the gravimetric method because a significant amount of penetrant may desorb when the sample is removed from the solution. Fourth, the MIR-FTIR technique may provide *in situ* information about chemical reactions (e.g., polymer degradation) or physical interactions (e.g., hydrogen bonding) that may occur between the polymer and the diffusant. And lastly, it is also possible to use this method to study the influences of defects and microstructure inherently formed during the film application and formation. In this paper, we present a method based on MIR-FTIR to measure the diffusion coefficients of liquid in polymer films applied to a substrate. The experimental method described here was designed primarily to measure *in situ* liquid water mass uptake and diffusion based on sorption kinetics, but it can also be suitable for vapors, or for other liquids.

THEORETICAL

We use a model derived from the second Fick law in which the diffusion coefficient is constant.[8] The general equation for the diffusing species reduces to[9]:

$$\frac{\partial C}{\partial t} = D\,\frac{\partial^2 C}{\partial z^2} \tag{1}$$

where C is the diffusant concentration and D the diffusion coefficient. A classical solution for a polymer film of thickness $2L$ placed in an infinite bath of diffusant is given by[9]:

$$\frac{C}{C_s} = 1 - \frac{4}{\pi}\sum_{n=0}^{\infty}\frac{(-1)^n}{2n+1}\exp\left[\frac{-D(2n+1)^2\pi^2 t}{4L^2}\right] *\cos\left[\frac{(2n+1)\pi z}{2L}\right] \tag{2}$$

with boundary conditions being zero initial concentration of diffusant at $t = 0$, and the concentration at both surfaces ($z = L$ and $z = -L$) being instantaneously established at a concentration C_s at any time. Equation (2) gives the concentration of diffusant at any depth in the film, and at any time. Using the gravimetric method, the mass of the sorbed diffusant is measured as a function of time. Integrating eq. (2) over the thickness of the film to obtain the sorbed mass as a function of time yields:

$$\frac{M_t}{M_\infty} = 1 - \sum_{n=0}^{\infty}\frac{8}{(2n+1)^2\pi^2} \times \exp\left[\frac{-D(2n+1)^2\pi^2 t}{4L^2}\right] \tag{3}$$

where M_t is the sorbed mass at time t, and M_∞ the sorbed mass at equilibrium. For short periods, $M_t/M_\infty \leq 0.5$, eq. (3) can be written as:

$$\frac{M_t}{M_\infty} = \frac{2}{L}\left(\frac{D}{\pi}\right)^{1/2} t^{1/2} \tag{4}$$

Under these conditions, for longer periods of time, the solution of eq. (3) can be written:

$$\frac{M_t}{M_\infty} = 1 - \frac{8}{\pi^2}\exp\left(\frac{-D\pi^2 t}{4L^2}\right) \tag{5}$$

The MIR-FTIR technique does not directly give the mass of diffusant at a given depth, but pro-

vides absorbance (A_t) data, which are proportional to the instantaneous mass of the diffusant (M_t). The measurement of such mass in the polymeric film by MIR-FTIR spectroscopy depends on the interaction between the sample and the evanescent wave produced upon total reflection within the internal reflection element (IRE). Such an interaction causes the attenuation of propagating infrared beam. When a polymer film is exposed to a diffusant, the latter can enter the polymer and interact with the evanescent wave and be detected. The substrate in this case is an IRE having a refractive index higher than those of polymeric coating and diffusant.

The electric field strength, E, of the evanescent wave decays exponentially on penetrating the surface layer of a sample, as expressed by eq. (6):

$$E = E_0 \exp\left(-\frac{z}{d_p}\right) \tag{6}$$

where E_0 is the amplitude of the evanescent wave at the surface $z = 0$, and d_p the depth at which the initial amplitude E_0 has decreased to $1/e$ of its surface value. For nonabsorbing and weakly absorbing materials d_p, is commonly known as the "penetration depth" and is given by[10]:

$$d_p = \frac{\lambda}{2n_2\pi\sqrt{\sin^2\theta - \left(\frac{n_1}{n_2}\right)^2}} \tag{7}$$

where λ is the wavelength of the infrared radiation and θ the incident angle; n_1 and n_2 are the refractive indices of the sample and IRE, respectively.

Considering a film of thickness $2L$ deposited on the IRE and analyzed by FTIR-MIR, the corresponding absorbance A can be given by[8]:

$$A = \int_0^{2L} e^{(-2z/d_p)} \cdot dzN \frac{\varepsilon}{I_0} CE_0^2 \tag{8}$$

where ε is the absorption coefficient of diffusant, N the number of reflections into the IRE in contact with the sample, C the concentration of diffusant, I_0 the intensity of the incident light, and E_0 the amplitude of the evanescent wave at the surface ($z = L$).

Since the intensity of an infrared absorption band is proportional to the concentration by the Beer–Lambert law, the Fickian concentration profile [eq. (2)] can be inserted into eq. (8). The result of integration is given by eq. (9).

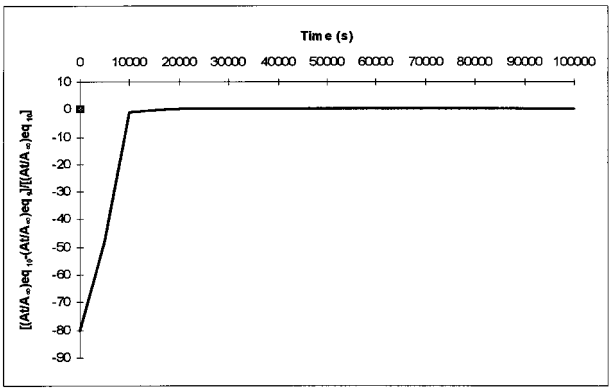

Figure 1 Comparison between the absorbance ratios calculated from eqs. (9) and (10).

$$\frac{A_t}{A_\infty} = 1 - \frac{8\gamma}{\pi[1 - \exp(-2\gamma L)]} \times \sum_{n=0}^{\infty}\left[\frac{\exp(g)[f\exp(-2\gamma L) + (-1)^n(2\gamma)]}{(2n+1)(4\gamma^2 + f^2)}\right] \tag{9}$$

where

$$g = \frac{-D(2n+1)^2\pi^2 t}{4L^2}, \quad \gamma = \frac{1}{d_p}, \quad \text{and } f = \frac{(2n+1)\pi}{2L}$$

Equation (9) is analogous to eq. (3) used in sorption gravimetric experiments. A_∞ represents the absorbance at equilibrium and is analogous to M_∞. If all terms in the series beyond the first one ($n = 1$) are eliminated, eq. (9) can be simplified and so:

$$\frac{A_t}{A_\infty} = 1 - \frac{8\gamma}{\pi[1 - \exp(-2\gamma L)]} * \left[\frac{\exp\left(\frac{-D\pi^2 t}{4L^2}\right) * \left(\frac{\pi}{2L}\exp(-2\gamma L) + (2\gamma)\right)}{\left(4\gamma^2 + \frac{\pi}{4L^2}\right)}\right] \tag{10}$$

The comparison between the absorbance ratios calculated from eqs. (9) and (10) is shown in Figure 1. It is clear that only the first-order term

Table I Characteristics of High and Low $\bar{M}_n$ PMMA Determined by Size Exclusion Chromatography

	High Molar Mass	Low Molar Mass
Number average molar mass	43,000 g mol^{-1}	8000 g mol^{-1}
Weight average molar mass	96,000 g mol^{-1}	14,000 g mol^{-1}
Polymolecularity index	2.2	1.7

Table II Characteristics of High and Low $\bar{M}_n$ PS Determined by Size Exclusion Chromatography

	High Molar Mass	Low Molar Mass
Number average molar mass	169,000 g mol^{-1}	93,000 g mol^{-1}
Weight average molar mass	339,000 g mol^{-1}	199,000 g mol^{-1}
Polymolecularity index	2.0	2.1

predominates in eq. (9). The significance of γ in the model depends on the experimental conditions. However, γ can be eliminated from eq. (10) if the experimental conditions given in expressions (11) and (12) are fulfilled.

$$4\gamma^2 \gg \frac{\pi^2}{4L^2} \tag{11}$$

$$\exp(-2\gamma L) \ll 1 \tag{12}$$

Under these conditions, eq. (10) can be reduced to the expression:

$$\ln\left(1 - \frac{A_t}{A_\infty}\right) = \ln\left(\frac{4}{\pi}\right) - \frac{D\pi^2}{4L^2}\,t \tag{13}$$

The diffusion coefficient D can be calculated by linear regression from experimental points. The value of D can also be determined from eq. (13) by plotting the logarithm of the absorbance data as a function of time. For period of time $<$ 2000 s, the slope of the curve gives D.

EXPERIMENTAL

Preparation of Polymer Films

The polymer films were obtained by casting solutions of poly(methyl methacrylate) (PMMA) or polystyrene (PS) in chloroform directly onto the lower surface of the internal reflection element (IRE). This operation was followed by solvent evaporation (8 h under ambient atmosphere and 2 h under vacuum). The refractive indices of PMMA and PS films were 1.4 and 1.5, respectively, as determined from reflectivity measurements at various incidence angles. The molecular weights were measured by size exclusion chromatography, and the results are presented in Tables I and II. PMMA and PS materials give relatively simple infrared absorption spectra. This fact minimizes the possibility of spectral interference between the polymer film and the diffusant. The coating thickness of dry films was measured using a micrometer. The thickness of each coating was reported as the average of three measurements.

Experimental Setup

The substrates IRE were cut from ZnS pieces (at dimensions 46 $\times$ 20 $\times$ 2 mm) and beveled at 22.5° in order to allow reflections under 45° incidence. Under these conditions, the infrared beam produces 23 internal reflections within the IRE. Figure 2 presents the specimen configuration and experimental setup. The cell body was made of poly(tetrafluoroethylene) and mirrors of gold-coated silicon.

FTIR Analysis

For the applications reported in this paper, the cell was placed in a FTIR spectrometer equipped with a liquid nitrogen-cooled mercury cadmium

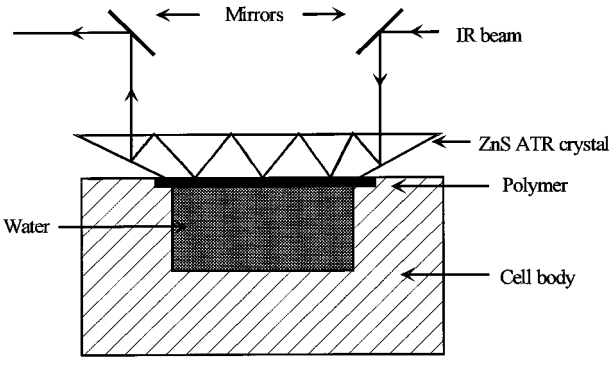

Figure 2 Schematic of the MIR-FTIR cell.

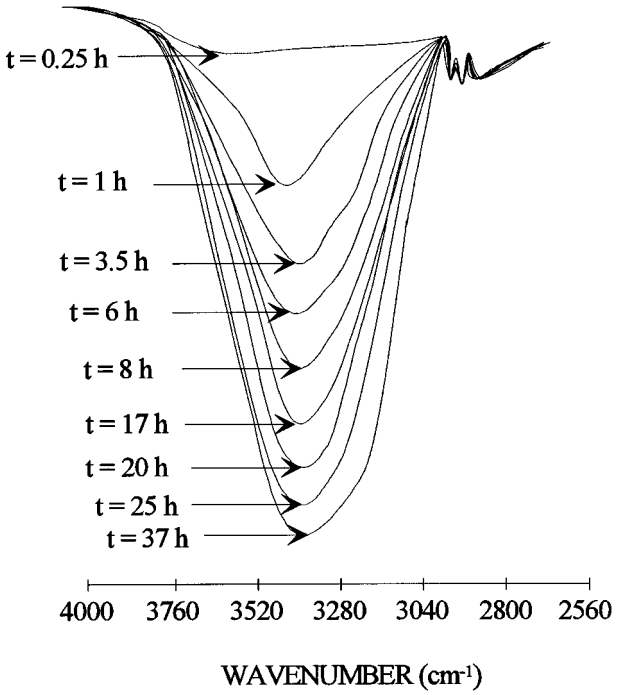

Figure 3 Sequence of time-evolved spectra from a PMMA sample of high molecular weight (43,000 g mol^{-1}) on a ZnS substrate exposed to water.

telluride detector. Before filling the cell with water, an MIR-FTIR spectrum was recorded, which was used as the background spectrum. Typically, 128 scans were collected at a resolution of 4 cm^{-1}. The diffusion of water into polymer films was measured by analyzing the absorbance change of the OH stretching peak. Peak area integrated from 3050 to 3700 cm^{-1} was used to express the intensity.

RESULTS AND DISCUSSION

Figure 3 displays MIR-FTIR spectra in the 2750 cm^{-1} to 4000 cm^{-1} region for a PMMA film applied to a ZnS substrate exposed to water for different times. The film has a thickness of 380 μm and an average molar mass $\bar{M}_n$ of 43,000 g mol^{-1}. These spectra are due to water molecules, as verified by the MIR-FTIR spectrum of liquid water in contact with a polymer-free substrate and using the same cell. Figure 4 shows the normalized absorbance (A_t/A_∞) versus square root of time. These data can be used for the determination of the diffusion coefficient. Unlike the gravimetric sorption experiments, we observe a "time lag" for this specimen before the FTIR absorbance was detected. This time represents the time required for water to diffuse through the film and reach the coating/substrate interfacial region. Such a time lag has been used by some authors[4,11] to determine the value of D.

The diffusion coefficients are determined (Table III) by fitting experimental data to curves corresponding to eqs. (10) and (13). Values obtained are in good agreement with those given in the literature for the same polymers[12] using gravimetry technique and for other polymers using the same FTIR technique but analyzed by the time lag approach[4] (Table III). The conformity to a Fickian behavior of this film can be inferred from the good agreement between the value determined with eq. (10) and experimental data as shown graphically in Figure 5. To further confirm this observation the reduced sorption curves, namely A_t/A_∞ against $t^{1/2}/2L$, were plotted. If the diffusion is Fickian, the reduced sorption curves should coincide for films of different thickness.[13] This is the case for the high $\bar{M}_n$ PMMA film because their reduced sorption curves for the 380 and 260 μm films coincide, as displayed in Figure 6.

For low $\bar{M}_n$ PMMA (8000 g mol^{-1}), the diffusion coefficients determined from eq. (10) and eq. (13) are somewhat different (Table III). These results suggest that the diffusion of water in low $\bar{M}_n$ PMMA probably did not follow a Fickian process. This is verified by the separation of the reduced sorption curves of films having different thicknesses, as illustrated in Figure 7.

Figure 8 presents the effect of molecular weight on the water transport process in PMMA films. For the same film thickness, the lower $\bar{M}_n$ material has a shorter initial time lag than that of the higher $\bar{M}_n$ film. This result is surprising because

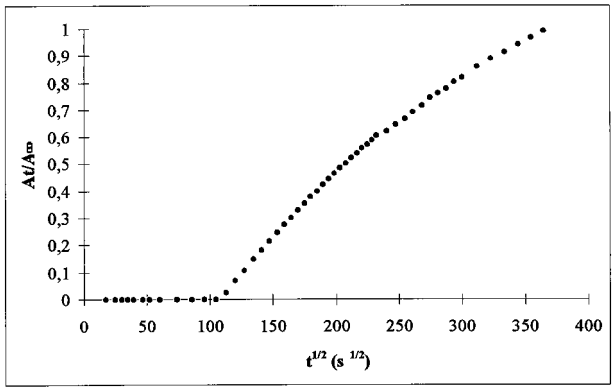

Figure 4 Normalized absorbance (A_t/A_∞) versus square root of time for a high $\bar{M}_n$ (43,000 g mol^{-1}) PMMA film.

Table III Value of the Diffusion Coefficient for Different Polymers

D^*10^8 ($cm^2\ s^{-1}$)	Polymer	Temperature (°C)	Reference
1.27 ± 0.13	PMMA [high $\bar{M}_n$, eq. (10)]	25	This article
1.28 ± 0.12	PMMA [high $\bar{M}_n$, eq. (13)]	25	This article
1.09 ± 0.11	PMMA [low $\bar{M}_n$, eq. (10)]	25	This article
1.35 ± 0.14	PMMA [low $\bar{M}_n$, eq. (13)]	25	This article
1	PMMA	21	12
1.58	PMMA	30	12
1.99	PMMA	34	12
2.3	PVC	30	22
4.3	PVA	25	23

several studies have reported that the diffusion coefficient as well as the process of sorption and permeation in polymers are independent of the molecular weight.[14–16] The observed effect of molar mass on the behavior of water transport in PMMA may be explained by the diffusion process in polymers, which consists of two steps: binding at an adsorbed site and moving from one site to the next. Unless the molecular weight is so low that the effects of chain end are appreciable, the second step should not be affected by an increase of molecular weight.[16] However, the residence time at each binding site (first step) depends on, among other factors, the strength of the association between the diffusant and the binding site: the weaker the association the shorter the residence time. For water in PMMA, the binding sites are the polar groups, such as C═O and C—O, and each adsorbed water molecule probably bonds to at least two such groups, as observed in biopolymers.[18]

The difference in the degree of bonding between water and C═O groups of PMMA having two different molar masses was investigated by the MIR-FTIR technique. Figure 9 displays the C═O stretching band of a high $\bar{M}_n$ film before and after water exposure. After the exposure, the C═O band has shifted from 1730 cm^{-1} to 1723 cm^{-1}. A shift to lower frequency of an infrared stretching band is generally due to an increase in the degree of hydrogen bonding.[19] No such shift is observed for the C═O band for the low $\bar{M}_n$ film. These results suggest that the association between a water molecule and the C═O in the high $\bar{M}_n$ PMMA is stronger than that in the low $\bar{M}_n$ film, and this difference is probably responsible for the distinction in the time lag between the two samples. The variation in the degree of hydrogen bonding between water and C═O group of PMMA at different molar masses cannot be explained by a density difference between the two PMMA, because as it can be seen in (Table IV), the density doesn't seem to be a function of the molar mass for PMMA.

One explanation for these data can be that the

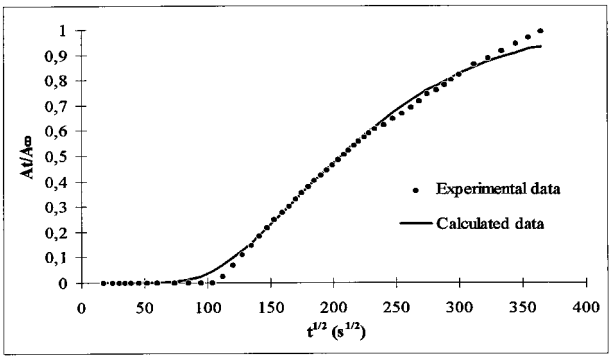

Figure 5 Comparison of diffusion data calculated with eq. (10) and experimental data, for a high $\bar{M}_n$ (43,000 g mol^{-1}) PMMA film.

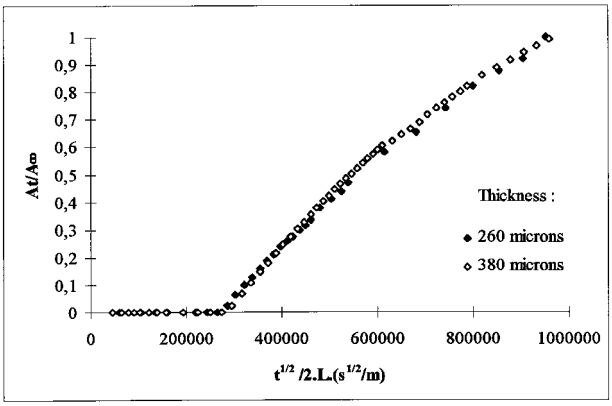

Figure 6 Reduced sorption curves for of high $\bar{M}_n$ (43,000 g mol^{-1}) PMMA exposed to water.

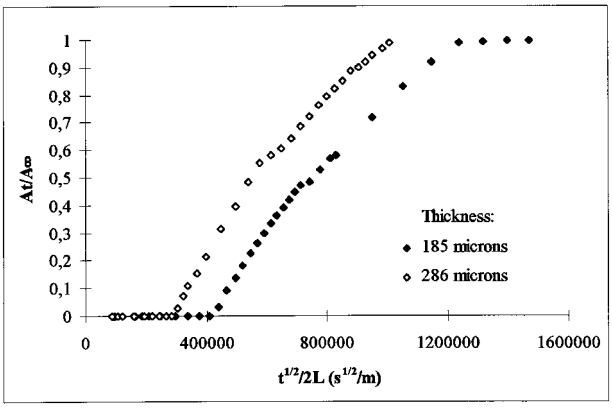

Figure 7 Reduced sorption curves for PMMA films of low $\bar{M}_n$ (8000 g mol^{-1}) exposed to water.

higher degree of hydrogen bonding between water and high $\bar{M}_n$ PMMA could be expressed in terms of accessibility of the bonding sites and nature of the chains packing. From a morphological point of view, low $\bar{M}_n$ PMMA, whose molar mass is under the critical mass[20] M_{cr} = 30,000 g mol^{-1}, has probably a more ordered structure, due to a higher mobility of its chains, than high $\bar{M}_n$ PMMA in which chains can become entangled and lead to more conformations.

The study of water diffusion in PS films shows a different behavior as compared to that observed for PMMA material. The transport of water from the environment to the interfacial region for the PS film was fast, and no time lag was observed (see Fig. 10). This phenomenon occurred in both low and high molecular weight films. The diffusion coefficient D, calculated by least squares fitting from experimental values, is $\sim 6.0 \times 10^{-8}$ cm^2 s^{-1}. The determination of D allows a comparison between experimental data with values obtained by calculation. These results are displayed in Figure 10, which indicates that the diffusion of water in PS films did not follow a Fickian process. The rapid non-Fickian transport of water in the PS film was probably due to the presence of defects in the bulk of this material. To verify this postulation, a transmission electron microscopy (TEM) analysis of PS thin sections was conducted. Figure 11 presents a typical TEM micrograph of a thin slice (<100 nm) microtomed from a thick PS film. This figure reveals many defects and pores in the film. This observation confirms a water transport process influenced by the de-

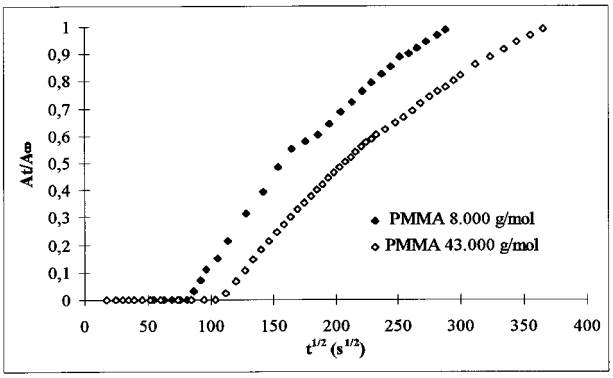

Figure 8 Curves of absorbance ratios versus exposure time for a high (43,000 g mol^{-1}) and a low (8000 g mol^{-1}) $\bar{M}_n$ PMMA film.

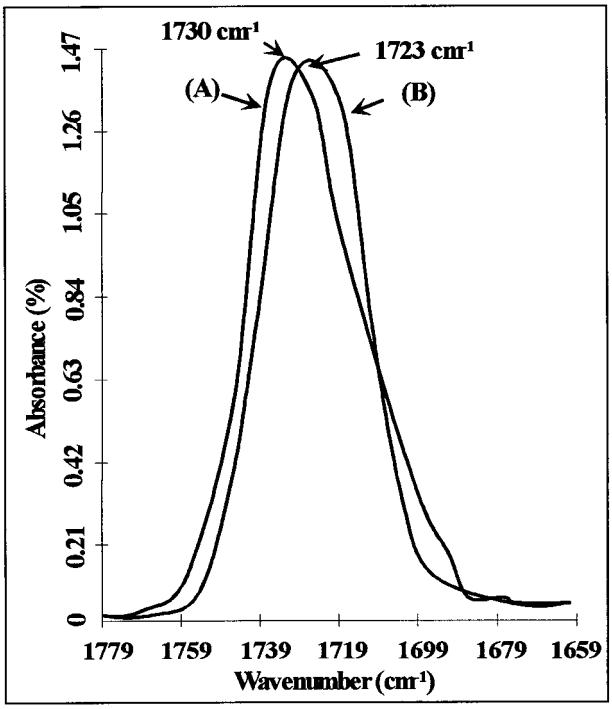

Figure 9 Carbonyl absorption band ν(C=O) from PMMA of high $\bar{M}_n$ (43,000 g mol^{-1}) before (A) and after (B) water exposure.

Table IV Value of the Specific Volume for PMMA of Different $\bar{M}_n$

$\bar{M}_n$ (g·mol^{-1})	$\bar{V}$ (cm^3 g^{-1})
10,000	0.8446
25,000	0.8460
40,000	0.8446
100,000	0.8453

Ambient conditions (see ref. 24).

fects in the films and explains the lack of conformity to the Fick law.

These data show the impossibility to get accurate values for the diffusion coefficient of water in PS, due to the fact that no PS film could be obtained without defects.

SUMMARY AND CONCLUSIONS

The results presented here were selected from an extensive study on the adhesion loss of PS and PMMA coatings subjected to water aggression.[21] The main objective of this paper was to demonstrate the applicability of a spectroscopic method based on multiple internal reflection Fourier transform infrared spectroscopy (MIR-FTIR) to study the transport of a solvent, water, in a polymer film applied to a substrate. The unique aspect of this technique is its ability to provide *in situ* information on the transport process, without any external perturbation of the specimens. The use of classical diffusion laws, adapted to a MIR-FTIR investigation, allows a determination of the diffusion processes and coefficients. The polymer films selected in this study exhibit different diffusion characteristics. High molecular weight PMMA follows a Fickian process. For low molecular weight PMMA, the diffusion is no longer Fickian, which is attributable to a weaker interaction of water molecules with polar groups of the polymer. The transport of water in PS films also did not obey the diffusion law, and this is due to the presence of defects in the films.

The results presented in this paper demonstrated that MIR-FTIR technique can be used effectively to characterize the water transport process in a polymer film applied to a substrate. Such information can be used to provide the diffusion coefficient of water in polymeric coatings and to study the effects of film microstructure and application parameters on the transport of water or solvents in polymeric films.

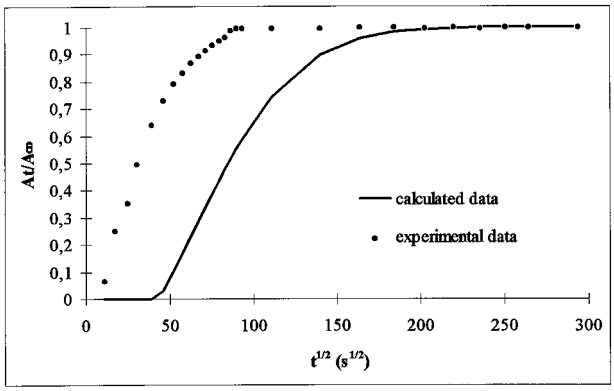

Figure 10 Comparison of experimental diffusion data and data calculated with eq. (10) for a polystyrene film of high $\bar{M}_n$ (169,000 g mol^{-1}).

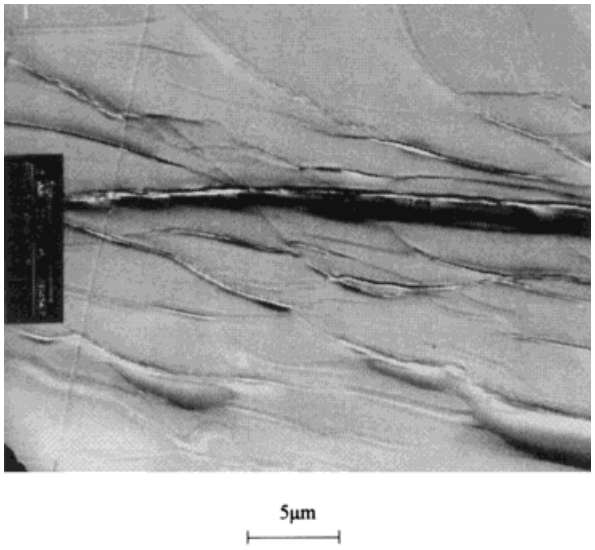

Figure 11 Transmission electron micrograph of a polystyrene film.

The authors acknowledge the Center for Electron Microscopy and the Laboratory of Plastics Materials and Biomaterials from the University of Lyon for the characterization of the polymer films.

REFERENCES

1. C. M. Balik and J. R. Xu, *J. Appl. Polym. Sci.,* **52,** 975 (1994).
2. N. L. Thomas and A. H. Windle, *Polymer,* **22,** 627 (1991).
3. T. P. Skourlis and R. L. McCullough, *J. Appl. Polym. Sci.,* **52,** 1241 (1994).
4. T. Nguyen, D. Bentz, and E. Byrd, *J. Coat. Technol.,* **67,** 37 (1995).
5. T. Asada, K. Inoue, and S. Onogi, *Polymer,* **8,** 21 (1976).
6. R. M. Felder and G. S. Huvard, in *Methods of Experimental Physics,* R. A. Fava, Ed., Academic Press, New York, 1980, p. 315.
7. J. R. Xu and C. M. Balik, *Appl. Spectr.,* **42,** 8, 1543 (1988).
8. G. T. Fieldson and T. A. Barbari, *Polymer,* **34,** 1146 (1993).

9. J. Crank, *The Mathematics of Diffusion,* 2nd ed., Oxford University Press, London, 1975.
10. N. J. Harrick, *Internal Reflection Spectroscopy,* Wiley Interscience, New York, 1967.
11. C. E. Rogers, *Polymer Permeability,* J. Comyn, Ed., Elsevier Applied Science Publishers, New York, 1985, p. 23.
12. F. Bueche, *J. Polym. Sci.,* **14,** 414 (1954).
13. J. Comyn, *Durability of Structural Adhesives,* A. J. Kinloch, Ed., Applied Science Publishers, London, 1983.
14. G. S. Park, *J. Polym. Sci.,* **11,** 97 (1953).
15. M. G. Hayes and G. S. Park, *Trans. Faraday Soc.,* **51,** 1134 (1955).
16. K. Uerreiter, *Diffusion in Polymers,* J. Crank and G. S. Park, Eds., Academic Press, London, 1968, p. 233.
17. H. Fujita, *Diffusion in Polymers,* J. Crank and G. S. Park, Eds., Academic Press, London, 1968, p. 75.
18. H. J. C. Berendsen, *Water: A Comprehensive Treatise,* F. Franks, Ed., Plenum Press, London, 1975, p. 5, 293.
19. G. C. Pigmental and A. L. McCellan, *Ann. Rev. Phys. Chem.,* **22,** 3247 (1971).
20. D. W. Van Krevelen, *Properties of Polymers,* Elsevier, Amsterdam, 1990.
21. I. Linossier, F. Gaillard, and M. Romand, *Proceedings of the 19th Annual Meeting of the Adhesion Society,* T. C. Ward, Ed., The Adhesion Society Inc., Feb. 18–21, 1996, Myrtle Beach, South Carolina.
22. A. M. Thomas, *Appl. Chem., London,* **1,** 141 (1951).
23. A. Kishimoto, E. Maekawa, and H. Fujita, *Bull. Chem. Soc. Jpn.,* **33,** 988 (1960).
24. P. Zoller and D. Walsh, *Standard Pressure-Volume-Temperature Data for Polymers,* Technomic, Lancaster, 1995, p. 145.